

# Porous Metal–Organic Framework with Coordinatively Unsaturated Mn<sup>II</sup> Sites: Sorption Properties for Various Gases

Hoi Ri Moon, Norihito Kobayashi, and Myunghyun Paik Suh\*

Department of Chemistry, Seoul National University, Seoul 151-747, Republic of Korea

Received June 29, 2006

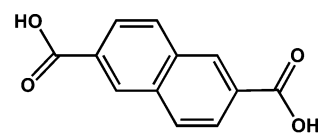
A 3D porous metal–organic framework generating 1D channels, [Mn(NDC)(DEF)]<sub>n</sub> (**1**), has been prepared from the solvothermal reaction of Mn<sup>II</sup> and 2,6-naphthalenedicarboxylic acid (H<sub>2</sub>NDC) in diethylformamide (DEF). When DEF molecules coordinating Mn<sup>II</sup>, which occupy the channels, are removed from **1** by heating the crystal of **1** at 250 °C under vacuum for 18 h, structural change occurs as evidenced by X-ray powder diffraction patterns. Desolvated solid [Mn(NDC)]<sub>n</sub> (**2**), which contains coordinatively unsaturated Mn<sup>II</sup> sites, reveals remarkable sorption capabilities for N<sub>2</sub>, H<sub>2</sub>, CO<sub>2</sub>, and CH<sub>4</sub> gases and exhibits type I sorption behavior indicative of permanent microporosity.

## Introduction

Open metal–organic frameworks (MOFs) have received great attention because of their diverse architectures and potential applications in molecular adsorption and separation processes,<sup>1,2</sup> ion exchange,<sup>3</sup> catalysis,<sup>4</sup> sensor technology,<sup>2,4,5</sup> and optoelectronics.<sup>6</sup> For the modular construction of MOFs, secondary building units (SBUs) with specific geometry have often been employed,<sup>2,7,8</sup> and they make the design and prediction of molecular architectures simple and easy. For example, the SBU of an octahedral-shaped Zn<sub>4</sub>O cluster, which is formed from the solvothermal reaction of Zn<sup>2+</sup> and carboxylic acid, furnishes 3D porous frameworks.<sup>2,8</sup> In particular, MOFs with coordinatively unsaturated metal sites

(CUMSs) are important because they are expected to be effective heterogeneous catalysts.<sup>9</sup> However, the chance of finding a MOF that contains CUMSs and yet exhibits permanent porosity is extremely rare<sup>10</sup> because the open structure easily collapses upon removal of the coordinating solvent molecules.

Here we report a 3D open MOF [Mn(NDC)(DEF)]<sub>n</sub> (**1**; NDC<sup>2-</sup> = 2,6-naphthalenedicarboxylate; DEF = diethylformamide) and its desolvated solid [Mn(NDC)]<sub>n</sub> (**2**). Solid **2** contains coordinatively unsaturated Mn<sup>II</sup> sites as evidenced by elemental analysis, IR spectra, thermogravimetric analysis (TGA), and X-ray powder diffraction (XRPD) data as well as coordination ability of water molecules. It adsorbs some important gases such as N<sub>2</sub>, H<sub>2</sub>, CO<sub>2</sub>, and CH<sub>4</sub>, exhibiting permanent microporosity.



2,6-naphthalenedicarboxylic acid (H<sub>2</sub>NDC)

## Experimental Section

**Preparation of [Mn(NDC)(DEF)]<sub>n</sub> (**1**).** Mn(NO<sub>3</sub>)<sub>2</sub>·nH<sub>2</sub>O (0.18 g, ca. 1.0 mmol) and 2,6-naphthalenedicarboxylic acid (H<sub>2</sub>NDC; 0.22 g, 1.0 mmol) were dissolved in diethylformamide (DEF; 7 mL). The solution was placed in a Teflon vessel within the

\* To whom correspondence should be addressed. E-mail: mpsuh@snu.ac.kr.

- (1) (a) Choi, H. J.; Suh, M. P. *J. Am. Chem. Soc.* **2004**, *126*, 15844–15851. (b) Suh, M. P.; Ko, J. W.; Choi, H. J. *J. Am. Chem. Soc.* **2002**, *124*, 10976–10977. (c) Min, K. S.; Suh, M. P. *Chem.—Eur. J.* **2001**, *7*, 303–313. (d) Lee, E. Y.; Suh, M. P. *Angew. Chem., Int. Ed.* **2004**, *43*, 2798–2801. (e) Choi, H. J.; Lee, T. S.; Suh, M. P. *Angew. Chem., Int. Ed.* **1999**, *38*, 1405–1408. (f) Kitaura, K. R.; Akiyama, G.; Kitagawa, S. *Angew. Chem., Int. Ed.* **2003**, *42*, 428–431. (g) Yaghi, O. M.; O’Keeffe, M.; Ockwig, N. W.; Chae, H. K.; Eddaoudi, M.; Kim, J. *Nature* **2003**, *423*, 705–714.
- (2) Lee, E. Y.; Jang, S. Y.; Suh, M. P. *J. Am. Chem. Soc.* **2005**, *127*, 6374–6381.
- (3) (a) Min, K. S.; Suh, M. P. *J. Am. Chem. Soc.* **2000**, *122*, 6834–6840. (b) Yaghi, O. M.; Li, H. *J. Am. Chem. Soc.* **1996**, *118*, 295–296.
- (4) (a) Wu, C. D.; Hu, A.; Zhang, L.; Lin, W. *J. Am. Chem. Soc.* **2005**, *127*, 8940–8941. (b) Gomez-Lor, B.; Gutierrez-Puebla, E.; Iglesias, M.; Monge, M. A.; Ruiz-Valero, C.; Snejko, N. *Chem. Mater.* **2005**, *17*, 2568–2573. (c) Sawaki, T.; Aoyama, Y. *J. Am. Chem. Soc.* **1999**, *121*, 4793–4798.
- (5) (a) Albrecht, M.; Lutz, M.; Spek, A. L.; van Koten, G. *Nature* **2000**, *406*, 970–974. (b) Real, J. A.; Andrés, E.; Muñoz, M. C.; Julve, M.; Granier, T.; Bousseksou, A.; Varret, F. *Science* **1995**, *268*, 265–267. (c) Beauvais, L. G.; Shores, M. P.; Long, J. R. *J. Am. Chem. Soc.* **2000**, *122*, 2763–2772.
- (6) Evans, O. R.; Lin, W. *Chem. Mater.* **2001**, *13*, 2705–2712.

- (7) (a) Eddaoudi, M.; Moler, D. B.; Li, H.; Chen, B.; Reineke, T. M.; O’Keeffe, M.; Yaghi, O. M. *Acc. Chem. Res.* **2001**, *34*, 319–330. (b) Murugavel, R.; Walawalkar, M. G.; Dan, M.; Roesky, H. W.; Rao, C. N. R. *Acc. Chem. Res.* **2004**, *37*, 763–774. (c) Serre, C.; Millange, F.; Surlblé, S.; Férey, G. *Angew. Chem., Int. Ed.* **2004**, *43*, 6286–6289. (d) Rosi, N. L.; Kim, J.; Eddaoudi, M.; Chen, B.; O’Keeffe, M.; Yaghi, O. M. *J. Am. Chem. Soc.* **2005**, *127*, 1504–1518.

autoclave, heated at 105 °C for 24 h, and then cooled to room temperature. Pale-yellowish block-shaped crystals were formed, which were filtered off, washed with DEF, and dried in air. Yield: 88%. FT-IR (Nujol mull):  $\nu_{\text{C=O(DEF)}}$ , 1648;  $\nu_{\text{O=C=O}}$ , 1611(s), 1554(s) cm<sup>-1</sup>. UV/vis (diffuse reflectance,  $\lambda_{\text{max}}$ ): 330, 285 nm. Anal. Calcd for MnC<sub>17</sub>H<sub>17</sub>NO<sub>5</sub>: C, 55.15; H, 4.63; N, 3.78. Found: C, 55.17; H, 4.71; N, 3.50.

**Preparation of [Mn(NDC)]<sub>n</sub> (2).** Solid **1** was heated in a Schlenk tube at 250 °C under vacuum for 18 h. FT-IR (Nujol mull):  $\nu_{\text{O=C=O}}$ , 1602(s), 1552(s) cm<sup>-1</sup>. UV/vis (diffuse reflectance,  $\lambda_{\text{max}}$ ): 357, 289 nm. Anal. Calcd for MnC<sub>12</sub>H<sub>6</sub>O<sub>4</sub>: C, 53.56; H, 2.25; N, 0.00. Found: C, 52.54; H, 2.43.

**Gas Sorption Measurements.** The gas adsorption–desorption experiments were performed using an automated micropore gas analyzer Autosorb-1 (Quantachrome Instruments). The sample was pre-desolvated in a Schlenk tube at 250 °C under vacuum for 18 h. An exactly measured amount of the pre-desolvated sample was introduced into the gas sorption instrument, and the outgassing process was carried out under vacuum at 150 °C for 3 h. After the gas sorption measurement, the weight was measured again. The outgassing procedure was repeated at 150 °C on the same sample between experiments for ca. 2 h. All gases used were of 99.999% purity. The N<sub>2</sub> gas sorption isotherm for the desolvated solid was monitored at 77 K by using liquid N<sub>2</sub> at each equilibrium pressure by the static volumetric method. The H<sub>2</sub> gas sorption isotherm was measured at 77 K by a similar procedure. Sorption isotherms for CO<sub>2</sub> and CH<sub>4</sub> were measured at both 195 and 273 K by using an acetone/dry ice slush and an ice/water bath, respectively. The sorption properties including the pore volume, pore size, and surface area were analyzed using Autosorb 1 for Windows 1.24 software.

**X-ray Crystallography.** The single crystal of **1** was sealed in a glass capillary together with the mother liquor. Diffraction data were collected on an Enraf Nonius Kappa CCD diffractometer with graphite-monochromated Mo K $\alpha$  radiation ( $\lambda = 0.71073$  Å). Preliminary orientation matrixes and unit cell parameters were obtained from the peaks of the first 10 frames and then refined using the whole data set. Frames were integrated and corrected for Lorentz and polarization effects by using *DENZO*.<sup>11</sup> The scaling and global refinement of crystal parameters were performed by *SCALEPACK*.<sup>11</sup> No absorption correction was made. The crystal structure was solved by direct methods<sup>12</sup> and refined by full-matrix least-squares refinement using the *SHELXL-97* computer program.<sup>13</sup> The positions of all non-H atoms were refined with anisotropic displacement factors. The H atoms were positioned geometrically and refined using a riding model. The crystallographic data and selected bond distances and angles are summarized in Tables 1 and 2.

**Table 1.** Crystallographic Data for **1**

formula	MnC <sub>17</sub> H <sub>17</sub> NO <sub>5</sub>
cryst syst	monoclinic
space group	<i>P</i> 2 <sub>1</sub> / <i>a</i>
fw	370.26
<i>a</i> , Å	7.535(5)
<i>b</i> , Å	21.513(5)
<i>c</i> , Å	10.466(5)
$\beta$ , deg	96.666(5)
<i>V</i> , Å <sup>3</sup>	1685.1(14)
<i>Z</i>	4
$\rho_{\text{calcd}}$ , g cm <sup>-3</sup>	1.459
temp, K	153(2)
$\lambda$ , Å	0.71073
$\mu$ , mm <sup>-1</sup>	0.809
GOF ( <i>F</i> <sup>2</sup> )	0.995
<i>F</i> (000)	746
reflns collected	6691
indep reflns	3771
completeness to $\theta_{\text{max}}$ , %	97.8
$\theta$ range for data collection, deg	3.3–27.48
diffraction limits ( <i>h</i> , <i>k</i> , <i>l</i> )	−9 ≤ <i>h</i> ≤ 9, −27 ≤ <i>k</i> ≤ 25, −13 ≤ <i>l</i> ≤ 13
refinement method	full-matrix least squares on <i>F</i> <sup>2</sup>
R1, <sup>a</sup> wR2 <sup>b</sup> [ <i>I</i> > 2 $\sigma$ ( <i>I</i> )]	0.0457, 0.0834
R1, <sup>a</sup> wR2 <sup>b</sup> (all data)	0.0995, 0.1108
largest peak, hole, eÅ <sup>-3</sup>	0.49, −0.333

<sup>a</sup> R1 =  $\sum||F_o| - |F_c||/\sum|F_o|$ . <sup>b</sup> wR2(*F*<sup>2</sup>) =  $[\sum w(F_o^2 - F_c^2)^2/\sum w(F_o^2)^2]^{1/2}$  where  $w = 1/[\sigma^2(F_o^2) + (0.0533P)^2 + (0.0000)P]$ ,  $P = (F_o^2 + 2F_c^2)/3$ .

**Table 2.** Selected Bond Distances (Å) and Angles (deg) for **1**<sup>a</sup>

Mn–O(1)	2.282(2)	Mn–O(2)	2.324(2)
Mn–O(2) <sup>i</sup>	2.145(2)	Mn–O(3)	2.080(2)
Mn–O(4) <sup>i</sup>	2.122(2)	Mn–O(5)	2.199(2)
O(1)–Mn–O(2)	56.9(1)	O(1)–Mn–O(2) <sup>i</sup>	106.2(1)
O(2)–Mn–O(3)	95.9(1)	O(2) <sup>i</sup> –Mn–O(3)	101.0(1)
O(1)–Mn–O(4) <sup>i</sup>	83.3(1)	O(2)–Mn–O(4) <sup>i</sup>	89.5(1)
O(2) <sup>i</sup> –Mn–O(4) <sup>i</sup>	89.5(1)	O(3)–Mn–O(4) <sup>i</sup>	99.8(1)
O(1)–Mn–O(5)	84.2(1)	O(2)–Mn–O(5)	91.0(1)
O(2) <sup>i</sup> –Mn–O(5)	85.5(1)	O(3)–Mn–O(5)	95.4(1)
O(1)–Mn–O(3)	152.7(1)	O(2)–Mn–O(2) <sup>i</sup>	163.0(1)
O(4) <sup>i</sup> –Mn–O(5)	164.7(1)		

<sup>a</sup> Symmetry transformations used to generate equivalent atoms: *i*, *x* + 1/2, 1/2 − *y*, *z*.

## Results and Discussion

**Preparation and X-ray Structure of 1.** Pale-yellowish block-shaped crystals of **1** were prepared by heating the DEF solutions of Mn(NO<sub>3</sub>)<sub>2</sub>·*n*H<sub>2</sub>O and H<sub>2</sub>NDC at 105 °C for 24 h. The X-ray crystal structure of **1** is shown in Figure 1. In **1**, Mn<sup>II</sup> ions are bridged by carboxylato groups in parts a and b of Chart 1 to form a 1D Mn<sup>II</sup> chain that extends along the *a* direction. The intrachain Mn–Mn distance is 3.805 Å. Each Mn<sup>II</sup> is coordinated with six O atoms that belong to four carboxylato groups and one DEF, showing pseudo-octahedral coordination geometry. The carboxylato group O(1)–C(6)–O(2) acts as a tridentate (Chart 1b) and forms a four-membered chelate ring with Mn [O(1)–Mn–O(2) angle, 56.9°]. The Mn–O distances range from 2.080 to 2.324 Å. The 1D Mn<sup>II</sup> chains are linked one to another via naphthalene rings of NDC<sup>2-</sup> to form a 3D framework that generates 1D channels of rhombic aperture with diagonal lengths of 21.5 Å × 10.5 Å. The effective window size of the channels is ca. 6.1 Å. The planes made of naphthalene rings of NDC<sup>2-</sup> run parallel to the (011) and (0 $\bar{1}$ 1) planes

- (8) (a) Eddaoudi, M.; Kim, J.; Rosi, N.; Vodak, D.; Wachter, J.; O’Keeffe, M.; Yaghi, O. M. *Science* **2002**, 295, 469–472. (b) Kim, J.; Chen, B.; Reineke, T. M.; Li, H.; Eddaoudi, M.; Moler, D. B.; O’Keeffe, M.; Yaghi, O. M. *J. Am. Chem. Soc.* **2001**, 123, 8239–8247.
- (9) Kitagawa, S.; Kitaura, R.; Noro, S. *Angew. Chem., Int. Ed.* **2004**, 43, 2334–2375.
- (10) (a) Chen, B.; Eddaoudi, M.; Reineke, T. M.; Kampf, J. W.; O’Keeffe, M.; Yaghi, O. M. *J. Am. Chem. Soc.* **2000**, 122, 11559–11560. (b) Li, H.; Davis, C. E.; Groy, T. L.; Kelley, D. G.; Yaghi, O. M. *J. Am. Chem. Soc.* **1998**, 120, 2186–2187. (c) Chen, B.; Ockwig, N. W.; Millward, A. R.; Contreras, D. S.; Yaghi, O. M. *Angew. Chem., Int. Ed.* **2005**, 44, 4745–4749.
- (11) Otwinowsky, Z.; Minor, W. In *Processing of X-ray Diffraction Data Collected in Oscillation Mode, Methods in Enzymology*; Carter, C. W., Sweet, R. M., Eds.; Academic Press: New York, 1996; Vol. 276, pp 307–326.
- (12) Sheldrick, G. M. *Acta Crystallogr.* **1990**, A46, 467.
- (13) Sheldrick, G. M. *SHELXL97, Program for the crystal structure refinement*; University of Göttingen: Göttingen, Germany, 1997.

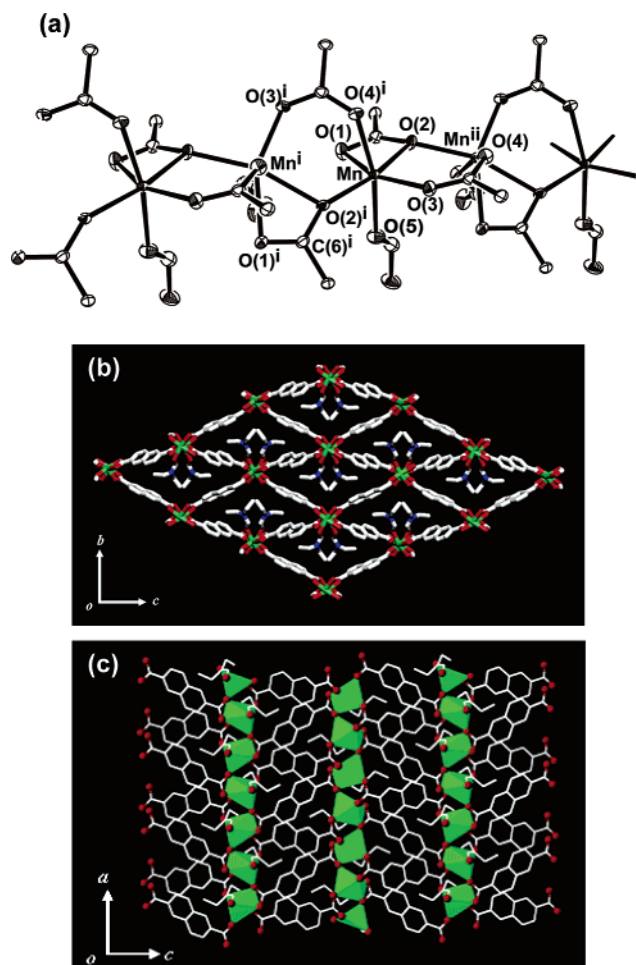
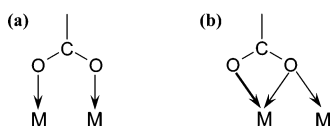


**Figure 1.** (a) ORTEP drawing of **1** with atomic numbering scheme (thermal ellipsoids at 30% probability). Symmetry operations: i,  $x + 1/2$ ,  $1/2 - y$ ,  $z$ ; ii,  $x - 1/2$ ,  $1/2 - y$ ,  $z$ . Naphthalene rings of NDC<sup>2-</sup> and ethyl groups of coordinating DEF molecules are omitted for clarity. (b) Top view showing a 3D framework generating 1D channels running along the *a* direction. The DEF molecules coordinating Mn<sup>II</sup> ions occupy the channels. (c) Side view showing that Mn<sup>II</sup> 1D chains are linked with each other via the naphthalene rings of NDC<sup>2-</sup>. Color code: Mn, green; C, white; O, red; N, blue.

#### Chart 1. Bridging Modes of Carboxylato Groups in **1**



and meet across at the 1D Mn<sup>II</sup> chains with a dihedral angle of 50.5°. Although 3D frameworks have been constructed from NDC<sup>2-</sup> and other metal ions such as Mg<sup>2+</sup>,<sup>14</sup> Zn<sup>2+</sup>,<sup>14</sup> and Ni<sup>2+</sup>,<sup>15</sup> they show structures different from that of **1**. The void space of the channels is filled with DEF molecules coordinating Mn<sup>II</sup> ions. The void volume that may be generated after removal of the coordinating DEF molecules is 42.1% of the total volume as estimated by PLATON.<sup>16</sup>

Framework **1** is insoluble in water and any organic solvents. TGA data indicate that all coordinating DEF

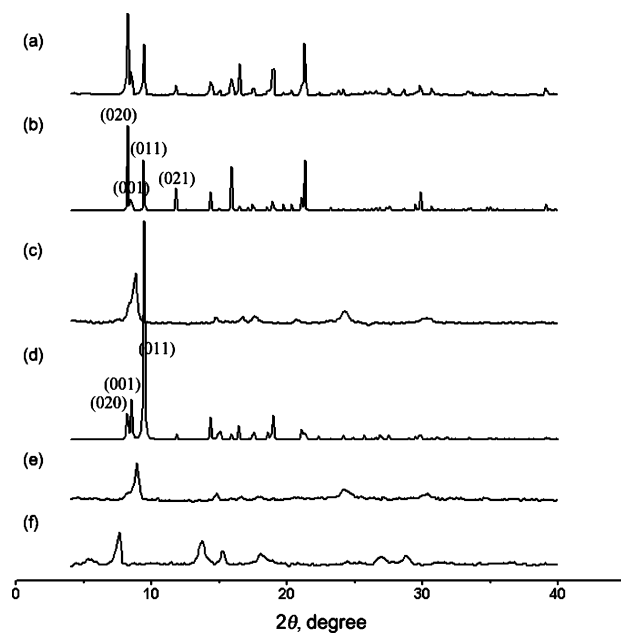


**Figure 2.** XRPD patterns for (a) as-synthesized **1**, (b) that simulated based on X-ray single-crystal data of **1**, (c) **2** prepared by drying **1** at 250 °C under vacuum for 18 h, (d) that simulated based on X-ray single-crystal data of **1** by omitting DEF, (e) a solid isolated after immersion of **2** in DEF for 24 h, and (f) a solid isolated after exposure of **2** to water vapor for 3 days.

molecules can be removed from **1** at 250 °C (calcd 27%; found 26%) and no chemical decomposition occurs up to 450 °C.

**Preparation and Properties of 2.** By heating of the crystals of **1** at 250 °C under vacuum for 18 h, desolvated solid **2** was prepared, in which DEF molecules coordinating Mn<sup>II</sup> ions are completely removed as evidenced by elemental analysis data, IR spectra, and TGA results. Crystal **2** lost transparency and crystallinity, and thus its X-ray crystal structure could not be determined.

In Figure 2, the XRPD patterns of **1** and **2** are compared. The XRPD pattern of **1** is coincident with the simulated pattern derived from the X-ray crystal data, implying that the bulk sample is the same as the single crystal. The XRPD pattern of desolvated solid **2** is different from that of **1** as well as the simulated pattern of **1** without DEF, indicating that the framework structure changes upon removal of the coordinating DEF molecules. In addition, the XRPD pattern of **1** could not be regenerated even when **2** was immersed in DEF for 24 h to 3 days, indicating that the original structure can hardly be restored once the coordinating DEF molecules are removed. Elemental analysis data indicate that, even after immersion in DEF, the solid does not contain DEF. It is revealed by Rietveld refinement<sup>17</sup> that the dramatic change in the XRPD pattern is caused by the reduction of effective pore apertures. The simulated framework structure of **2** was obtained by Rietveld refinement, which was performed until its XRPD pattern matched with the measured pattern of **2** (see the Supporting Information). The simulated structure indicates that the rhombic aperture of the channel

(14) Dinca, M.; Long, J. R. *J. Am. Chem. Soc.* **2005**, *127*, 9376–9377.

(15) Kongshaug, K. O.; Fjellvag, H. *Solid State Sci.* **2003**, *5*, 303–310.

(16) Spek, A. L. *PLATON99, A Multipurpose Crystallographic Tool*; Utrecht University: Utrecht, The Netherlands, 1999.

(17) The refinement was performed by using *X-cell evaluation software* that was supplied by Accelrys Software Inc.

in **2** is significantly squeezed (rhombic angle, 36.3° in **2** vs 50.5° in **1**) even though the 3D structure is retained, and thus the effective diameter of the aperture of **2** is reduced (ca. 6 Å in **1** vs 4 Å in **2**). Therefore, the difficulty of reintroduction of DEF in the channels in **2** can be explained by the reduced aperture.

Recently, we have revealed the reversible rearrangement of the coordination geometry of the metal ions in MOF to a stable coordinatively saturated one upon removal of coordinating solvent molecules.<sup>18</sup> However, in the present study, the possibility of rearrangement of the coordination geometry of Mn<sup>II</sup> from octahedral geometry to a coordinatively saturated trigonal bipyramid instead of a coordinatively unsaturated square pyramid can be ruled out because of the four-membered chelate ring around Mn<sup>II</sup>, based on the model study.

Because **2** contains accessible coordination sites on Mn<sup>II</sup>, it adsorbs water vapor when solid **2** is exposed to water vapor for 3 days, which results in a XRPD pattern that is different from either **1** or **2**. The shift of the peak at  $2\theta = 8.8^\circ$  in **2** to a lower angle region ( $7.6^\circ$ ) indicates the expansion of the channel size upon exposure to water vapor. The IR spectrum showed a new water peak at  $3392\text{ cm}^{-1}$ , and the elemental analysis data indicated that two water molecules per Mn<sup>II</sup> ion were included in the solid. Anal. Calcd for Mn(NDC)·2H<sub>2</sub>O: C, 47.23; H, 3.30. Found: C, 46.59; H, 3.36. It is assumed that a water molecule coordinates to the vacant coordination site of each Mn<sup>II</sup>, and one water molecule per formula unit of **2** is included in the channel, which gives rise to a framework structure different from either **1** or **2**. The XRPD pattern of **2** is not altered up to 400 °C (see the Supporting Information), indicating the high thermal stability of framework structure **2**.

**Gas Sorption Properties.** To verify the porosity of **2**, which contains coordinatively unsaturated Mn<sup>II</sup> ions, the gas sorption capabilities were measured for N<sub>2</sub>, H<sub>2</sub>, CO<sub>2</sub>, and CH<sub>4</sub> gases. Interestingly, solid **2** adsorbs these gases with remarkable storage capacity (Figure 3 and Table 3). Considering the kinetic diameters of the gases, H<sub>2</sub> (2.8 Å), CO<sub>2</sub> (3.3 Å), N<sub>2</sub> (3.64 Å), and CH<sub>4</sub> (3.8 Å),<sup>19</sup> and assuming that the framework structure does not change upon gas adsorption, it can be assumed that the pore opening in **2** is greater than 3.8 Å in diameter.

Desolvated solid **2** adsorbs N<sub>2</sub> gas to show a reversible type I isotherm, indicating the permanent microporosity of **2**. The gas sorption shows a little hysteresis between sorption/desorption curves, suggesting a small amount of mesoporosity present in the desolvated material **2**, which is attributed to nanosized intercrystalline voids or mesopores within the mosaic pseudomorphs that remain after desolvation.<sup>20</sup> Solid **2** adsorbs 8.8 wt % of N<sub>2</sub> at 77 K and 0.95 atm (68 cm<sup>3</sup>/g at STP). The Langmuir surface area is estimated as 191 m<sup>2</sup>/g,

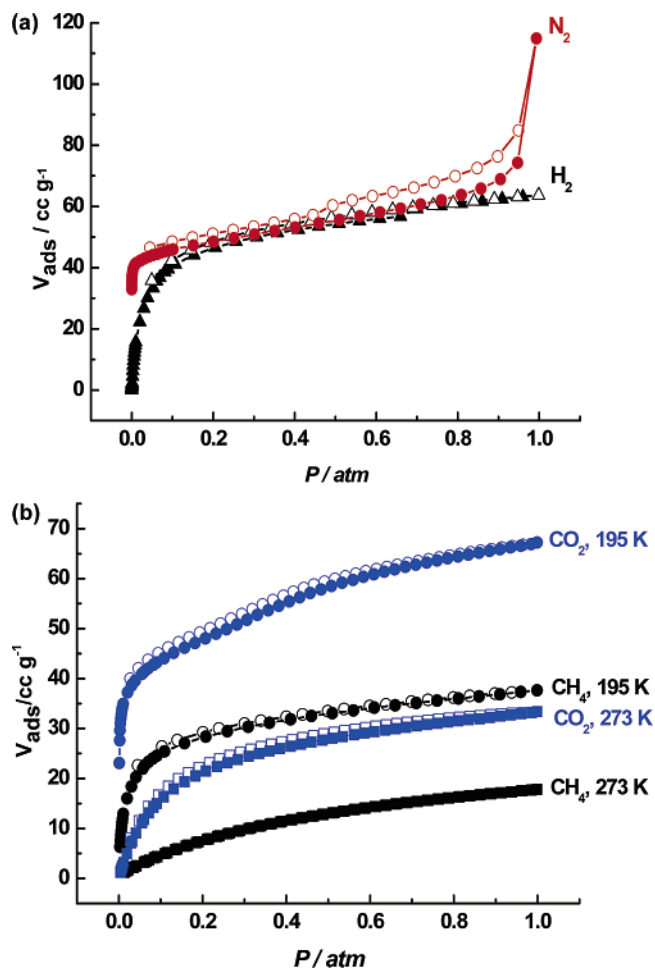


**Figure 3.** Gas sorption isotherms for **2**: (a) N<sub>2</sub> and H<sub>2</sub> at 77 K; (b) CO<sub>2</sub> (blue) and CH<sub>4</sub> (black) at 195 K (circle) and 273 K (square).  $P_0(\text{N}_2) = 760$  Torr. Filled shapes: adsorption. Open shapes: desorption.

**Table 3.** Gas Sorption Data for Various Gases

gas	$T$ (K)	Langmuir surface area of <b>2</b> (m <sup>2</sup> /g)	pore volume of <b>2</b> (cm <sup>3</sup> /g)	mmol of gas/g of <b>2</b>	wt % gas	gas adsorbed per volume of host, <sup>a</sup> cm <sup>3</sup> /cm <sup>3</sup>
N <sub>2</sub>	77	191	0.068	3.1	8.8	72
H <sub>2</sub>	77			2.8	0.57	68
CO <sub>2</sub>	195	227	0.11	3.0	13	71
CO <sub>2</sub>	273			1.5	6.6	35
CH <sub>4</sub>	195			1.7	2.7	40
CH <sub>4</sub>	273			0.8	1.3	19

<sup>a</sup> The values are calculated by using the density of **2** (1.06 g/cm<sup>3</sup>), assuming that the cell volume of **1** is retained in **2**, even though the XRPD pattern of **2** is different from that of **1**.

which is comparable to those of another Mn<sup>II</sup> framework, Mn(HCO<sub>2</sub>)<sub>2</sub>· $\frac{1}{3}$ C<sub>4</sub>H<sub>8</sub>O<sub>2</sub> (ca. 240 m<sup>2</sup>/g),<sup>21</sup> and of microporous zeolites.<sup>19,22</sup> The pore volume estimated by applying the Dubinin–Radushkevich equation is 0.068 cm<sup>3</sup>/g. With **2**, sorption/desorption cycles can be repeated many times, which is contrary to the common MOFs that collapse to a close-packed structure after the gas release.<sup>23</sup>

Solid **2** also adsorbs H<sub>2</sub> gas up to 0.57 wt % at 77 K and 1 atm (64 cm<sup>3</sup>/g at STP). This H<sub>2</sub> uptake capacity is much

(18) Cheon, Y. E.; Lee, E. Y.; Suh, M. P. Submitted.

(19) Beck, D. W. *Zeolite Molecular Sieves*; Wiley & Sons: New York, 1974.

(20) (a) Vishnyakov, A.; Ravikovitch, P. I.; Neimark, A. V.; Bulow, M.; Wang, O. M. *Nano Lett.* **2003**, *3*, 713–718. (b) Lee, J. Y.; Li, J.; Jagiello, J. J. *Solid State Chem.* **2005**, *178*, 2527–2532.

(21) Dybtsev, D.-N.; Chun, H.; Yoon, S. Y.; Kim, D.; Kim, K. *J. Am. Chem. Soc.* **2004**, *126*, 32–33.

(22) Choudhary, V. R.; Mayadevi, S. *Zeolites* **1996**, *17*, 501–507.

inferior to the materials that we published recently,<sup>1d,2</sup> [Ni-(cyclam)(bpydc)] and [Zn<sub>4</sub>O(NTB)<sub>2</sub>], which adsorb 1.1 and 1.9 wt % of H<sub>2</sub>, respectively. The value is rather comparable to that of ZSM-5 (0.7 wt %).<sup>24</sup> Compared to Mg<sub>3</sub>(NDC)<sub>3</sub>, which adsorbs 0.46 wt % at 77 K and 880 Torr,<sup>14</sup> the present Mn<sup>II</sup> framework shows 125% better H<sub>2</sub> storage capacity. The density of adsorbed H<sub>2</sub> at 77 K and 1 atm is 0.052 g/cm<sup>3</sup>, based on the pore volume estimated from the CO<sub>2</sub> sorption data at 195 K. This value is higher than those of any porous MOFs reported so far<sup>1d,2,21,25</sup> and is comparable to that of liquid H<sub>2</sub> (0.053 g/cm<sup>3</sup> at 30 K and 8.1 atm).<sup>26</sup> It should be noted here that the MOFs with CUMSs have been anticipated to show very high H<sub>2</sub> sorption because H<sub>2</sub> adsorption is regarded as a mixture of physi- and chemisorptions. However, the present result indicates that CUMSs in the MOF do not help the H<sub>2</sub> adsorption significantly.

Solid **2** shows a high CO<sub>2</sub> sorption capacity even at higher temperatures, 195 and 273 K. It adsorbs 13 wt % of CO<sub>2</sub> at 195 K and 1 atm (67.2 cm<sup>3</sup>/g at STP; Table 3). This value is comparable to that (12 wt %, 60.5 cm<sup>3</sup>/g at STP) of tris-*o*-phenylenedioxytriphosphazene (TPP) containing 1D channels with a similar diameter, which was reported as a high CO<sub>2</sub> storage material.<sup>27</sup> In the CO<sub>2</sub> sorption data also, there is some sort of hysteresis that extends to low pressures. This might originate from the swelling of the nonrigid porous structure of **2** or from the strong interactions of CO<sub>2</sub> molecules with the host solid **2**.<sup>28</sup> The storage capacity at 273 K is also considerably high, adsorbing 6.6 wt % at 1 atm (33.4 cm<sup>3</sup>/g at STP).

The gas isotherm for CH<sub>4</sub> measured at 195 K shows that **2** can store up to 2.7 wt % (37.7 cm<sup>3</sup>/g at STP), which exceeds those of inorganic zeolites<sup>19,22</sup> and organic material TPP (2.4 wt %, 43.9 cm<sup>3</sup>/cm<sup>3</sup>, 33.2 cm<sup>3</sup>/g at STP).<sup>27</sup> At 273 K, it stores 1.3 wt % (17.8 cm<sup>3</sup>/g at STP), which is higher than ca. 0.8 wt % (at 1 atm and 298 K) of ([{Cu(O<sub>2</sub>-CRCO<sub>2</sub>)-<sup>1/2</sup>TED}<sub>n</sub>] (R = 4,4'-C<sub>6</sub>H<sub>4</sub>C<sub>6</sub>H<sub>4</sub> or *trans*-C<sub>6</sub>H<sub>4</sub>CH=CH), which has a comparable channel size.<sup>29</sup>

The present results indicate that **2** shows much better adsorption capabilities for N<sub>2</sub> and CO<sub>2</sub> gases than H<sub>2</sub> in the low-pressure range (Figure 3). The removal of small amounts of contaminant gases from H<sub>2</sub> is important for the real use of H<sub>2</sub> as a fuel,<sup>30</sup> and this selectivity can be applied in the purification of H<sub>2</sub> gas. Furthermore, its adsorption capacity for CO<sub>2</sub> is higher than that of CH<sub>4</sub>, which can also be applied in CO<sub>2</sub> removal from the natural gas.

## Conclusion

We have prepared a 3D open MOF **1** from the simple solvothermal reaction of Mn(NO<sub>3</sub>)<sub>2</sub>·*n*H<sub>2</sub>O and H<sub>2</sub>NDC at 105 °C in DEF. Although **1** has no free space because the DEF molecules coordinating Mn<sup>II</sup> ions occupy the channels, they can be removed to obtain desolvated solid **2**. Solid **2** contains accessible coordination sites on Mn<sup>II</sup> sites, as evidenced by elemental analysis, IR, TGA, and XRPD data as well as the coordination ability of water molecules. Solid **2** reveals remarkable sorption capabilities for N<sub>2</sub>, H<sub>2</sub>, CO<sub>2</sub>, and CH<sub>4</sub> gases and exhibits type I sorption behavior indicative of permanent microporosity. Its adsorption capabilities of N<sub>2</sub>, CO<sub>2</sub>, and CH<sub>4</sub> gases over H<sub>2</sub> gas and that of CO<sub>2</sub> over CH<sub>4</sub> may be applied in the purification of H<sub>2</sub> gas and the removal of CO<sub>2</sub> from the natural gas.

**Acknowledgment.** This work was supported by Ministry of Commerce, Industry and Energy, Republic of Korea (Project 10022942) and by the SRC/ERC program of MOST/KOSEF (Grant R11-2005-008-03002-0). Dr. Norihito Kobayashi thanks the Brain Korea 21 program for the financial support.

**Supporting Information Available:** An ORTEP drawing of **1**, IR spectra and TGA/differential scanning calorimetry plots for **1** and **2**, the simulated structure of **2** obtained by Rietveld refinement and its XRPD pattern compared with that of **2**, temperature-dependent XRPD patterns of **1**, and an X-ray crystallographic file of **1** in CIF format. This material is available free of charge via the Internet at <http://pubs.acs.org>.

IC0611948

(29) Seki, K. *Chem. Commun.* **2001**, 1496–1497.

(30) Atwood, J. L.; Barbour, L. J.; Jerga, A. *Angew. Chem., Int. Ed.* **2004**, *43*, 2948–2950.

- (23) (a) Endo, K.; Sawaki, T.; Koyanagi, M.; Kobayashi, K.; Masuda, H.; Aoyama, Y. *J. Am. Chem. Soc.* **1995**, *117*, 8341–8352. (b) Cairra, M. R.; Nassimbeni, L. R.; Toda, F.; Vujovic, D. *J. Am. Chem. Soc.* **2000**, *122*, 9367–9372. (c) Saied, O.; Maris, T.; Wuest, J. D. *J. Am. Chem. Soc.* **2003**, *125*, 14956–14957.
- (24) (a) Nijkamp, M. G.; Raaymakers, J. E. M. J.; van Dillen, A. P.; de Jong, K. P. *Appl. Phys. A* **2001**, *72*, 619–623. (b) Weitkamp, J.; Fritz, M.; Ernst, S. *Int. J. Hydrogen Energy* **1995**, *20*, 967–970.
- (25) (a) Rosi, N. L.; Eckert, J.; Eddaoudi, M.; Vodak, D. T.; Kim, J.; O'Keeffe, M.; Yaghi, O. M. *Science* **2003**, *300*, 1127–1129. (b) Rowsell, J. C.; Millward, A. R.; Park, K. S.; Yaghi, O. M. *J. Am. Chem. Soc.* **2004**, *126*, 5666–5667. (c) Kaye, S. S.; Long, J. R. *J. Am. Chem. Soc.* **2005**, *127*, 6506–6507. (d) Lee, J. Y.; Pan, L.; Kelly, S. P.; Jagiello, J.; Emge, T. J.; Li, J. *Adv. Mater.* **2005**, *17*, 2703–2706.
- (26) National Institute of Standards and Technology homepage. <http://www.nist.gov/> (accessed February 2005).
- (27) Sozzani, P.; Bracco, S.; Comotti, A.; Ferretti, L.; Simonutti, R. *Angew. Chem., Int. Ed.* **2005**, *44*, 1816–1820.
- (28) (a) Lowell, S.; Shields, J. E.; Thomas, M. A.; Thommes, M. *Characterization of Porous Solids and Powders: Surface Area, Pore Size, and Density*; Kluwer Academic Publishers: Dordrecht, The Netherlands, July 2004; Chapter 4. (b) Sing, K. S. W.; Everett, D. H.; Haul, R. A. W.; Moscou, L.; Pierotti, R. A.; Rouquerol, J.; Siemieniewska, T. *Pure Appl. Chem.* **1985**, *57*, 603–619.